

***In silico* candidate variant and gene identification using inbred mouse strains**

Matthias Munz ^{Equal first author, 1}, **Mohammad Khodaygani** ^{Equal first author, 1}, **Zouhair Aherrahrou** ², **Hauke Busch** ^{Corresp., 1}, **Inken Wohlers** ^{Corresp. 1}

¹ Medical Systems Biology Division, Lübeck Institute of Experimental Dermatology and Institute for Cardiogenetics, University of Lübeck, Lübeck, Germany

² Institute for Cardiogenetics, University of Lübeck, Lübeck, Germany

Corresponding Authors: Hauke Busch, Inken Wohlers

Email address: Hauke.Busch@uni-luebeck.de, Inken.Wohlers@uni-luebeck.de

Mice are the most widely used animal model to study genotype to phenotype relationships. Inbred mice are genetically identical, which eliminates genetic heterogeneity and makes them particularly useful for genetic studies. Many different strains have been bred over decades and a vast amount of phenotypic data has been generated. In addition, recently whole genome sequencing-based genome-wide genotype data for many widely used inbred strains has been released. Here, we present an approach for *in silico* fine-mapping that uses genotypic data of 37 inbred mouse strains together with phenotypic data provided by the user to propose candidate variants and genes for the phenotype under study. Public genome-wide genotype data covering more than 74 million variant sites is queried efficiently in real-time to provide those variants that are compatible with the observed phenotype differences between strains. Variants can be filtered by molecular consequences and by corresponding molecular impact. Candidate gene lists can be generated from variant lists on the fly. Fine-mapping together with annotation or filtering of results is provided in a Bioconductor package called MouseFM. In order to characterize candidate variant lists under various settings, MouseFM was applied to two expression data sets across 20 inbred mouse strains, one from neutrophils and one from CD4⁺ T cells. Fine-mapping was assessed for about 10,000 genes, respectively, and identified candidate variants and haplotypes for many expression quantitative trait loci (eQTLs) reported previously based on these data. For albinism, MouseFM reports only one variant allele of moderate or high molecular impact that only albino mice share: a missense variant in the *Tyr* gene, reported previously to be causal for this phenotype. Performing *in silico* fine-mapping for interfrontal bone formation in mice using four strains with and five strains without interfrontal bone results in 12 genes. Of these, three are related to skull shaping abnormality. Finally performing fine-mapping for dystrophic cardiac calcification by comparing 9 strains showing the phenotype with 8 strains lacking it, we identify only one

moderate impact variant in the known causal gene *Abcc6*. In summary, this illustrates the benefit of using MouseFM for candidate variant and gene identification.

***In silico* candidate variant and gene identification using inbred mouse strains**

Matthias Munz^{1*}, Mohammad Khodaygani^{1*}, Zouhair Aherrahrou², Hauke Busch^{1#}, and Inken Wohlers^{1#}

¹**Medical Systems Biology Division, Lübeck Institute of Experimental Dermatology and Institute for Cardiogenetics, University of Lübeck, Lübeck, Germany**

²**Institute for Cardiogenetics, University of Lübeck, Lübeck, Germany**

***These authors contributed equally as co-first authors**

#**These authors contributed equally as co-last authors**

Corresponding author:

Hauke Busch and Inken Wohlers

Email address: hauke.busch@uni-luebeck.de and inken.wohlers@uni-luebeck.de

ABSTRACT

Mice are the most widely used animal model to study genotype to phenotype relationships. Inbred mice are genetically identical, which eliminates genetic heterogeneity and makes them particularly useful for genetic studies. Many different strains have been bred over decades and a vast amount of phenotypic data has been generated. In addition, recently whole genome sequencing-based genome-wide genotype data for many widely used inbred strains has been released. Here, we present an approach for *in silico* fine-mapping that uses genotypic data of 37 inbred mouse strains together with phenotypic data provided by the user to propose candidate variants and genes for the phenotype under study. Public genome-wide genotype data covering more than 74 million variant sites is queried efficiently in real-time to provide those variants that are compatible with the observed phenotype differences between strains. Variants can be filtered by molecular consequences and by corresponding molecular impact. Candidate gene lists can be generated from variant lists on the fly. Fine-mapping together with annotation or filtering of results is provided in a Bioconductor package called MouseFM. In order to characterize candidate variant lists under various settings, MouseFM was applied to two expression data sets across 20 inbred mouse strains, one from neutrophils and one from CD4⁺ T cells. Fine-mapping was assessed for about 10,000 genes, respectively, and identified candidate variants and haplotypes for many expression quantitative trait loci (eQTLs) reported previously based on these data. For albinism, MouseFM reports only one variant allele of moderate or high molecular impact that only albino mice share: a missense variant in the *Tyr* gene, reported previously to be causal for this phenotype. Performing *in silico* fine-mapping for interfrontal bone formation in mice using four strains with and five strains without interfrontal bone results in 12 genes. Of these, three are related to skull shaping abnormality. Finally performing fine-mapping for dystrophic cardiac calcification by comparing 9 strains showing the phenotype with 8 strains lacking it, we identify only one moderate impact variant in the known causal gene *Abcc6*. In summary, this illustrates the benefit of using MouseFM for candidate variant and gene identification.

INTRODUCTION

Mice are the most widely used animal models in research. Several factors such as small size, low cost of maintain, and fast reproduction as well as sharing disease phenotypes and physiological similarities with human makes them one of the most favourable animal models (Uhl and Warner, 2015). Inbred mouse strains are strains with all mice being genetically identical, i.e. clones, as a result of sibling mating for many generations, which results in eventually identical chromosome copies. When assessing genetic variance between mouse strains, the genome of the most commonly used inbred strain, called Black 6J (C57BL/6J) is typically used as reference and variants called with respect to the Black 6J mouse genome. For inbred mouse strains, variants are homozygous by design.

Grupe *et al.* in 2001 published impressive results utilizing first genome-wide genetic data for *in silico* fine-mapping of complex traits, “reducing the time required for analysis of such [inbred mouse]

48 models from many months down to milliseconds” (Grube et al., 2001). Darvasi commented on this
49 paper that in his opinion, the benefit of *in silico* fine-mapping lies in the analysis of monogenic traits
50 and in informing researchers prior to initiating traditional breeding-based studies. In 2007, with Cervino
51 *et al.*, he suggested to combine *in silico* mapping with expression information for gene prioritization
52 using 20,000 and 240,000 common variants, respectively (Cervino et al., 2007). Since then, the general
53 approach has been applied successfully and uncovered a number of genotype-phenotype relationships
54 in inbred mice (Liao et al., 2004; Zheng et al., 2012; Hall and Lammert, 2017; Mulligan et al., 2019).
55 Nonetheless, to the best of our knowledge, there is to date no tool publicly available that implements the
56 idea and which allows to analyze any phenotype of interest. Such a tool is particularly helpful now that
57 all genetic variation between all commonly used inbred strains is known at base pair resolution (Doran
58 et al., 2016; Keane et al., 2011).

59 At the same time, in the last years huge amounts of mouse phenotype data were generated, often
60 in collaborative efforts and systematically for many mouse strains. Examples are phenotyping under-
61 taken by the International Mouse Phenotyping Consortium (IMPC) (Dickinson et al., 2016)(Meehan
62 et al., 2017) or lately also the phenotyping of the expanded BXD family of mice (Ashbrook et al.,
63 2021). Data are publicly available in resources such as the mouse phenome database (MPD) (Bogue
64 et al., 2018) (<https://www.mousephenotype.org>) or the IMPC’s website (Dickinson et al.,
65 2016) (<https://phenome.jax.org>). Other websites such as Mouse Genome Informatics (MGI)
66 (<http://www.informatics.jax.org>) or GeneNetwork (Mulligan et al., 2017) (<https://www.genenetwork.org>) also house phenotype data together with web browser-based functionality to in-
67 vestigate genotype-phenotype relationships.

68 Several of the aforementioned resources allow the user to interactively query genotypes for 70 user-
69 selected inbred mouse strains for input genes or genetic regions. Moreover, the variant browser in
70 GeneNetwork allows also comparison of genotypes between strains, however, data can only be extracted
71 gene- or region-wise and is not accessible programmatically. No current resource thus provides the
72 functionality to extract genome-wide all variants that are different between two user-specified groups of
73 inbred mouse strains. Such information can be used for *in silico* fine-mapping and for the identification of
74 candidate genes and variants underlying a phenotypic trait. Further, such a catalog of genetic differences
75 between groups of strains is very useful prior to designing mouse breeding-based experiments e.g. for the
76 identification or fine-mapping of quantitative trait loci (QTL).
77

78 METHODS

79 Fine-mapping approach

80 Unlike previous approaches for *in silico* fine-mapping, here we are using whole genome sequencing-based
81 variant data and thus information on all single nucleotide variation present between inbred strains. Due to
82 the completeness of this variant data, we do not need to perform any statistical aggregation of variant data
83 over genetic loci, but simply report all variant sites with different alleles between two groups of inbred
84 strains. That is, we report all variant sites with alleles compatible with the observed phenotype difference,
85 see Figure 1 for an illustration.

86 In the case of a binary phenotype caused by a single variant, this causal variant is one of the variants
87 that has a different allele in those strains showing the phenotype compared to those strains lacking the
88 phenotype. This is the case for example for albinism and its underlying causal variant rs31191169, used
89 in Figure 1 for illustration and discussed later in detail.

90 This *in silico* fine-mapping approach can reduce the number of variants to a much smaller set of
91 variants that are compatible with a phenotype. The more inbred strains are phenotyped and used for
92 comparison, the more variants can be discarded because they are not compatible with the observed
93 phenotypic difference.

94 In the case of a quantitative phenotype, the fine-mapping can be performed in two ways. The first
95 option is to obtain genetic differences between strains showing the most extreme phenotypes. The second
96 option is binarization of the phenotype by applying a cutoff. Since in these cases allele differences of
97 variants affecting the trait may not be fully compatible with an artificially binarized phenotype, fine-
98 mapping is provided with an option that allows alleles of a certain number of strains to be incompatible
99 with the phenotype, see Figure 1 for an example.

100 Two important, related aspects need to be considered with respect to the *in silico* fine-mapping
101 approach implemented in MouseFM: (i) power and (ii) significance of the MouseFM candidates with

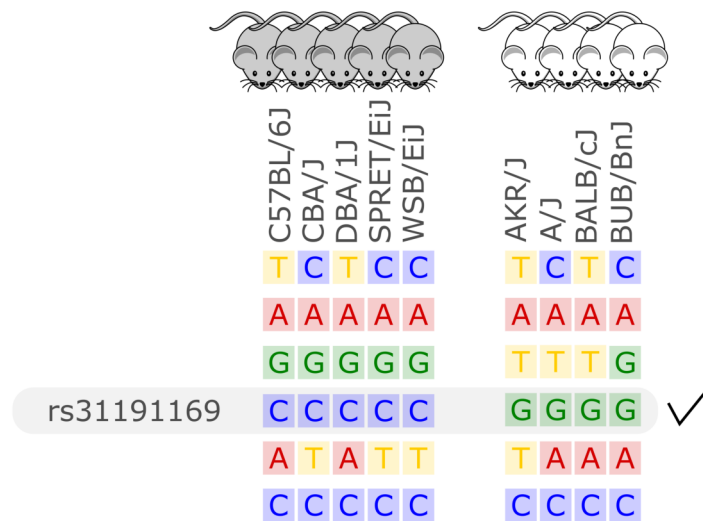


Figure 1. Illustration of the *in silico* fine-mapping approach. Every row represents a variant site and every column one inbred mouse strain. In this example, the phenotype is albinism and four strains are albinos and 5 are not. Displayed are six variants, but only one variant, rs31191169, has consistently different alleles between the albino and the other mice (G allele is here linked to albinism). With option `thr2=1` in the MouseFM package, one discordant strain would be allowed in the second strain group and the variant in the row above rs31191169 would also be returned.

102 respect to chance findings. With respect to (i): The suggested fine-mapping approach considerably gains
 103 power when increasing the number of inbred strains with phenotype data available. This is the result of an
 104 explosion of the number of possible genotype combinations across the analyzed strains. Figure 2 shows
 105 the number of possible genotype combinations. If, e.g. for a Mendelian trait, only one combination is
 106 compatible with the phenotype, it is increasingly unlikely to observe this combination by chance when the
 107 number of strains increases. Based on these theoretical considerations, we recommend using MouseFM
 108 for more than 8 phenotyped strains. The number of actual genotype combinations for a given set of
 109 inbred strains is less than the maximum depicted in Figure 2, because of kinship between strains. One
 110 favourable extreme are two phenotypic groups of overall closely related strains: only few variants differ
 111 between the groups and will be returned by MouseFM. The opposite extreme are groups of inbred strains
 112 closely related only within their phenotypic group, but not across groups: many variants will differ and be
 113 returned by MouseFM. With respect to (ii): For a low number of strains, a random split may result in
 114 a similar number of candidate variants compared to a split by phenotype and false-positive candidates
 115 increase. The important property is though, that in a split by phenotype, true positives will be among the
 116 candidates and once the number of phenotyped strains increases, the candidate set becomes smaller while
 117 still including true positives.

118 Variant data

119 The database used by this tool was created based on the genetic variants database of the Mouse Genomes
 120 Project (<https://www.sanger.ac.uk/science/data/mouse-genomes-project>) of the
 121 Wellcome Sanger Institute. It includes whole genome sequencing-based single nucleotide variants of
 122 36 inbred mouse strains which have been compiled by Keane et al. (2011), see ftp://ftp-mouse.sanger.ac.uk/REL-1502-BAM/sample_accessions.txt for the accession code and sources.
 123 This well designed set of inbred mouse strains for which genome-wide variant data is available in-
 124 cludes classical laboratory strains (C3H/HeJ, CBA/J, A/J, AKR/J, DBA/2J, LP/J, BALB/cJ, NZO/HILtJ,
 125 NOD/ShiLtJ), strains extensively used in knockout experiments (129S5SvEvBrd, 129P2/OlaHsd, 129S1/SvImJ,
 126 C57BL/6NJ), strains used commonly for a range of diseases (BUB/BnJ, C57BL/10J, C57BR/cdJ, C58/J,
 127 DBA/1J, I/LnJ, KK/HiJ, NZB/B1NJ, NZW/LacJ, RF/J, SEA/GnJ, ST/bJ) as well as wild-derived inbred
 128 strains from different mouse taxa (CAST/EiJ, PWK/PhJ, WSB/EiJ, SPRET/EiJ, MOLF/EiJ). Genome se-
 129 quencing, variant identification and characterization of 17 strains was performed by Keane et al. (2011) and
 130 of 13 strains by Doran et al. (2016). We downloaded the single nucleotide polymorphism (SNP) VCF file
 131

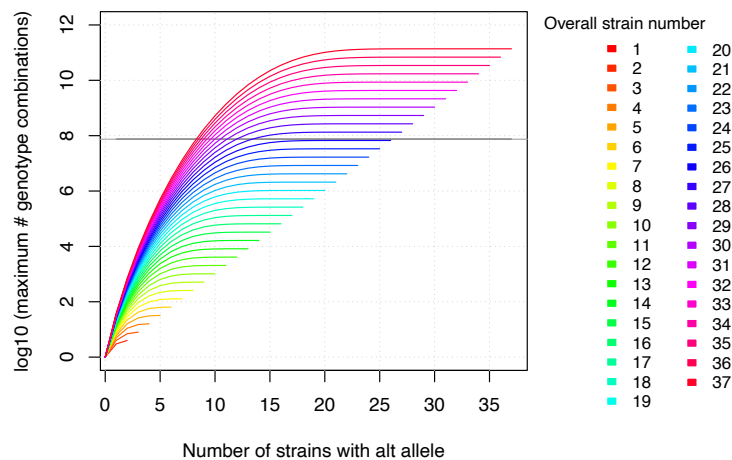


Figure 2. The maximum number of genotype combinations for an overall number of inbred strains n including up to k alternative alleles is given by $\sum_{k=1}^n \sum_{j=1}^k \binom{k}{j}$ and grows exponentially with respect to the overall number of inbred strains. Further the more evenly the alleles are divided among these overall strains, the larger the corresponding number of genotype combinations. The gray horizontal line denotes the number of variants in MouseFM ($n=74,480,058$). For more than 26 strains, the maximum number of genotype combinations are larger than the number of variant positions, and it is thus extremely unlikely to observe a phenotype-compatible combination by chance. For 10 and more strains, there is a maximum of more than 1000 genotype combinations, which reduces the probability of a phenotype-compatible combination already considerably. The number of actual, observed genotype combinations depends on the particular inbred strains used and, importantly, on their kinship.

132 ftp://ftp-mouse.sanger.ac.uk/current_snps/mgp.v5.merged.snps_all.dbSNP142.vcf.gz. Overall, it contains 78,767,736 SNPs, of which 74,873,854 are autosomal. The chromosomal positions map to the mouse reference genome assembly GRCm38 which is based on the Black 6J inbred mouse strain and by definition has no variant positions.

136 Low confidence, heterozygous, missing and multiallelic variants vary by strain, in sum they are typically less than 5% of the autosomal variants (Figure 3, Suppl. Table 1). Exceptions are for example the wild-derived inbred strains, for which variant genotypes excluded from the database reach a maximum of 11.5% for SPRET/EiJ. There are four strains that are markedly genetically different from each other and all remaining strains, these are the wild-derived, inbred strains CAST/EiJ, PWK/PhJ, SPRET/EiJ and MOLF/EiJ, see Figure 3A. These four strains also show the highest number of missing and multiallelic genotypes (Figure 3B and Suppl. Table 1).

143 Database

144 We re-annotated the source VCF file with Ensembl Variant Effect Predictor (VEP) v100 (McLaren et al., 2016) using a Docker container image (<https://github.com/matmu/vep>). For real-time retrieval of variants compatible with phenotypes under various filtering criteria, the variant data was loaded into a MySQL database. The database consists of a single table with columns for chromosomal locus, the reference SNP cluster ID (rsID), variant consequences based on a controlled vocabulary from the sequence ontology (Eilbeck et al., 2005), the consequence categorization into variant impacts “HIGH”, “MODERATE”, “LOW” or “MODIFIER” according to the Ensembl Variation database (Hunt et al., 2018) (see Suppl. Table 2 for details) and the genotypes (NULL = missing, low confidence, heterozygous or consisting of other alleles than reference or most frequent alternative allele; 0 = homozygous for the reference allele, 1 = homozygous for alternative allele). SNPs with exclusively NULL genotypes were not loaded into the database resulting in 74,480,058 autosomal SNVs that were finally added to our database. These have been annotated with overall 120,927,856 consequences, i.e. on average every variant has two annotated consequences. Figure 4 summarizes these consequence annotations stratified by impact; description of consequences and annotation counts are provided in Suppl. Table 2. Most annotations belong to impact category “MODIFIER” (99.4%). High impact annotations are rare, because they are typically deleterious (0.013%). Annotation with moderate impact consequences comprise only missense,

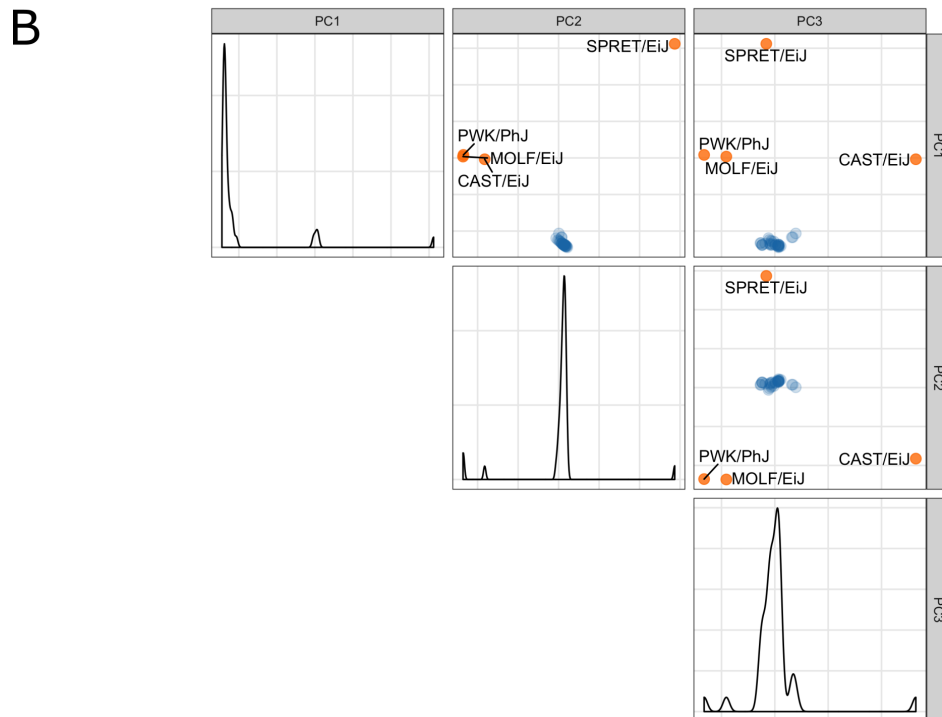
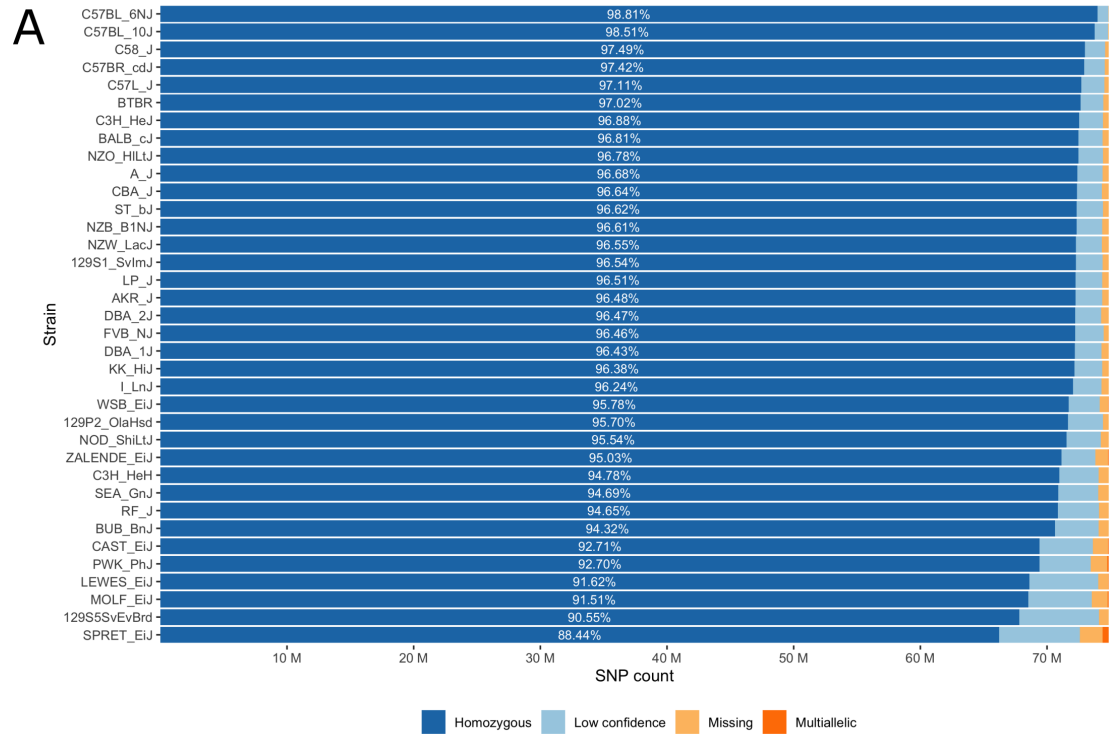


Figure 3. A) Inbred mouse strain autosomal SNP characteristics: The number of homozygous, low confidence, missing and multiallelic genotypes for 36 non-reference strains. For each strain, a SNP was checked for group membership in the order low confidence → missing → multiallelic → homozygous → heterozygous and was assigned to the first matching group. Since no SNP made it to the group with heterozygous genotypes it is not shown in the diagram. B) Principal component analysis shows four outlier inbred strains, CAST/EiJ, PWK/PhJ, SPRET/EiJ and MOLF/EiJ.

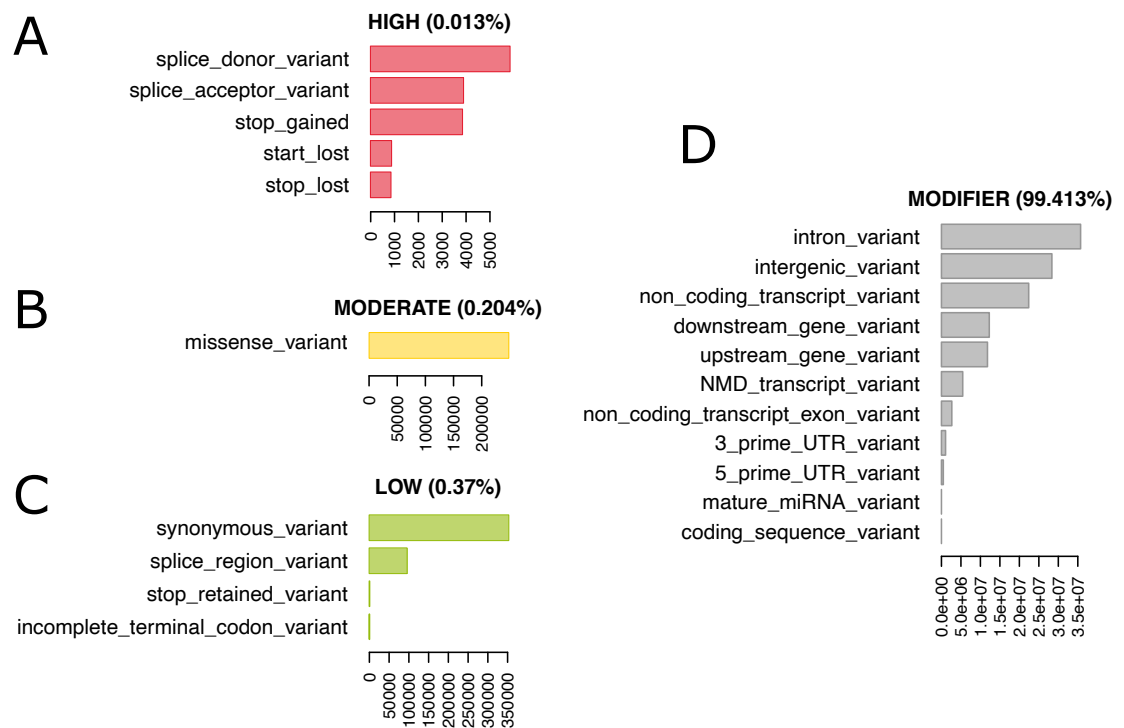


Figure 4. 74,480,058 variants have been annotated with 120,927,856 consequences. Shown here are the number of variants annotated with a given consequence, stratified by consequence impact. For description of consequence types see Suppl. Table 2. Both impact and consequence can be used for variant prioritization in MouseFM. A) Impact “HIGH”; B) Impact “MODERATE”; C) Impact “LOW”; D) Impact “MODIFIER”.

160 i.e. protein sequence altering variants contributing 0.204%. Low impact consequences are slightly more
 161 often annotated, amounting to 0.37%. Ensembl Variant Effect Predictor (VEP) annotation is loaded into
 162 the MouseFM database to allow for quick candidate ranking and filtering, which otherwise could not be
 163 performed in real-time. Additionally, all candidate variants can be retrieved unfiltered and independent of
 164 VEP predictions to allow for custom effect predictions, ranking and filtering.

165 **Bioconductor R package MouseFM**

166 Our fine-mapping approach was implemented as function `finemap` in the Bioconductor R package
 167 “MouseFM”. Bioconductor is a repository for open software for bioinformatics.

168 The function `finemap` takes as input two groups of inbred strains and one or more chromosomal
 169 regions on the GRCm38 assembly and returns a SNP list for which the homozygous genotypes are
 170 discordant between the two groups. Optionally, filters for variant consequence and impacts as well
 171 as a threshold for each group to allow for intra-group discordances can be passed. With function
 172 `annotate_mouse_genes` the SNP list can further be annotated with overlapping genes. Optionally,
 173 flanking regions can be passed.

174 The `finemap` function queries the genotype data from our backend server while function `annotate_mouse_genes`
 175 queries the Ensembl Rest Service (Yates et al., 2015). The repository containing the backend of the
 176 MouseFM tool, including the scripts of the ETL (Extract, transform, load) process and the webserver,
 177 is available at <https://github.com/matmu/MouseFM-Backend>. Following the repositories’
 178 instructions, users may also install the data base and server application on a local server.

179 The workflow and scripts to generate the MouseFM case study results are available at https://github.com/iwohlers/2020_mousefm_finemap.

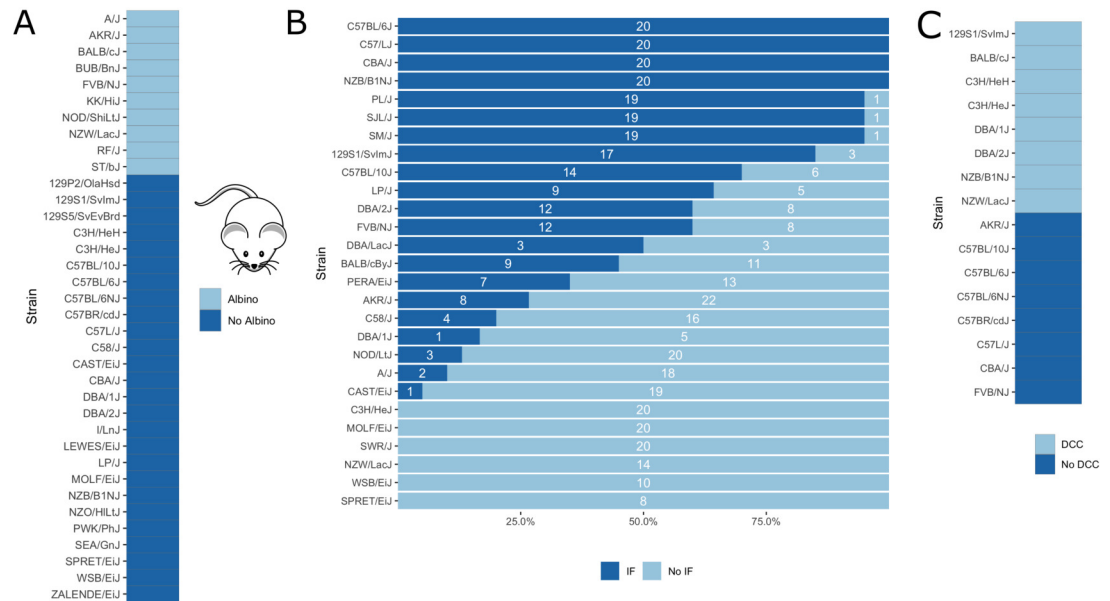


Figure 5. Visualization of mouse phenotypic data for which fine-mapping is performed. A) Binary inbred mouse strain phenotypic albinism. All or no mice of a strain are albinos; shown here is which strain belongs to which group. B) Quantitative inbred mouse strain phenotypic interfrontal bone (IF). Shown is the number of mice of the respective strain having an interfrontal bone (dark blue, IF) and not having an interfrontal bone (light blue, No IF). The interfrontal bone (IF) image is taken from (Zimmerman et al., 2019). C) Phenotypic cardiac dystrophic calcification (DCC). Five inbred strains show the phenotype and five strains lack it.

RESULTS

In order to characterize fine-mapping results of MouseFM for different numbers of strains and when applying the threshold parameter allowing phenotype-incompatible strains, we used a large gene expression data set. Such a data set contains both (i) genes with clear binary expression phenotype, likely caused by a *cis* variant or haplotype, (ii) cases with no or no binary difference in phenotype.

Further, as a proof of concept, we applied our *in silico* fine-mapping approach on three additional phenotypes: albinism, interfrontal bone formation and dystrophic cardiac calcification. Phenotypic data is illustrated in Figure 5.

Expression quantitative trait loci

MouseFM is particularly useful for detecting variants for which a large, binary effect on a trait can be observed. As such, it is useful for providing candidate variants affecting gene expression, i.e. expression quantitative trait loci (eQTLs). Here, we use two expression data sets to illustrate this use case as well as to investigate aspects of MouseFM candidate variant lists for a large number of traits with different characteristics. We use neutrophil and CD4⁺ T cell expression data from Mostafavi et al. (2014) generated in the context of an eQTL study by the Immunological Genome Project. This data is available for 39 inbred mouse strains of which 20 are part of MouseFM. Polymorphonuclear neutrophils (granulocytes) data is available under GEO Accession GSE60336, CD4⁺ T cell data under GSE60337. We downloaded the corresponding normalized expression data from <http://rstats.immgen.org/DataPage>. Of the strains used here, expression is assessed for two mice each, except for the Black 6J strain of which expression from five mice is available. Neutrophils further have expression for only one FVB mouse.

We read in the expression data and selected all mice from the 20 MouseFM strains (n=43 for CD4⁺ T cell; n= 42 for neutrophils). As Mostafavi et al. (2014), we keep only expressed genes using a cutoff of 120 expression on the intensity scale. This way, we obtain n=10,676 transcripts from 9,136 genes for T cells and n=10,137 transcripts from 8,687 genes for neutrophils, which is comparable to the numbers assessed by Mostafavi *et al.* using all 39 strains. Mostafavi et al. (2014) applied a well-designed dedicated

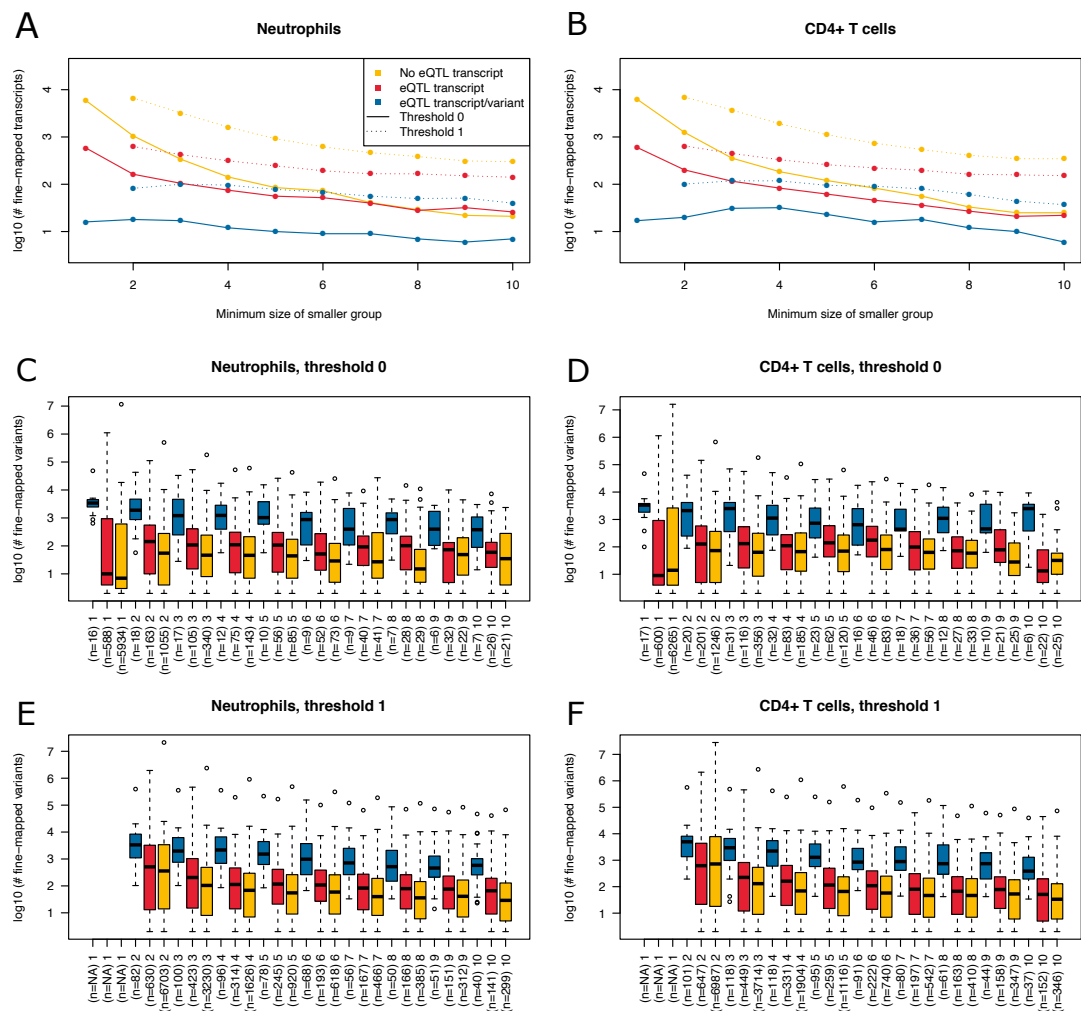


Figure 6. Summary of fine-mapping results for two expression data sets. Shown are numbers of fine-mapped transcripts and boxplots of fine-mapped variants for these transcripts. The subset of fine-mapped eQTL transcripts and variants according to Mostafavi et al. (2014) is colored blue, the subset of fine-mapped eQTL transcripts without reported eQTL variant according to Mostafavi et al. (2014) is colored red, remaining fine-mapped transcripts yellow. A) The number of successfully fine-mapped transcripts for the neutrophil data set on log₁₀ scale at different allowed minimum group sizes from 1 to 10. Solid lines denote a threshold of 0 incompatible strains, dashed lines denote a threshold of 1 of incompatible strains (thr1=1 and thr2=1). B) As A, but for CD4⁺ T cells. C) Boxplots of number of fine-mapped variants for the transcripts in A (threshold 0, i.e. solid lines) for different minimum group sizes from 1 to 10. D) As C, but for CD4⁺ T cells. E) Boxplots of number of fine-mapped variants for the transcripts in A (threshold 1, i.e. dashed lines and thr1=1 and thr2=1) for different minimum group sizes from 2 to 10. F) As E, but for CD4⁺ T cells.

206 statistical approach to identify and interpret *cis* eQTLs. Briefly, they introduce a metric called TV metric
207 to identify cases of bimodal gene expression and test SNPs within 1 Mb of the transcription start side using
208 a linear regression model. In our experimental setting, we also use a 1 Mb cutoff and aim to detect *cis*
209 eQTLs with MouseFM. For testing, genome-wide 96,779 SNPs were available in the study of Mostafavi
210 *et al.*. Overall, they identified 1,111 joint T cell and neutrophil eQTLs using $n=39$ strains. Assessment
211 with MouseFM uses about 74 million SNVs and can be considered somewhat an inverse approach to this
212 previous eQTL study: It is not testing expression differences for a SNP, but it needs as input a separation
213 of strains into two expression groups and identifies all compatible variants, if available. In order to assess
214 characteristics of fine-mapped variants of MouseFM, we use a very crude group separation based on
215 ordering strains using the mouse with minimum expression of a strain and then splitting at the rank of
216 maximum difference between median expression of all mice of strains with smaller rank compared to all
217 mice of strains with larger rank. We run MouseFM for smaller group size from 1 to 10. According to
218 theoretical expectation (cf. Figure 2), the number of cases in which MouseFM returns candidate variants
219 that are entirely compatible with phenotype decreases with increasing group size, see Figure 6A for
220 neutrophils and Figure 6B for $CD4^+$ T cells. At the same time, the proportion of previously detected
221 eQTL transcripts and the number of previously identified eQTL variants increases, because the probability
222 of chance findings decreases. The number of fine-mapped variants varies greatly, often being less than
223 ten but also often more than 100, see Figure 6C and Figure 6D, for neutrophils and T cells, respectively.
224 Cases, in which a previously reported eQTL variant was among the fine-mapped variants are comparably
225 few. In these cases, the number of fine-mapped variants tends to be larger than in those cases without a
226 previous eQTL variant among the fine-mapped variants. This effect is likely caused by the much smaller
227 number of variants assessed in the eQTL study – we observe a variant overlap only in cases of large
228 expression-compatible haplotypes. The overall number of fine-mapped variants is rather low, which may
229 be because of the crude group definition. We observe that group definition sometimes can be improved,
230 especially if expression is not clearly bimodal. Thus, it is useful to apply MouseFM with a threshold
231 allowing for a given number of incompatible strains. We here allow for one incompatible strain in the
232 first and one incompatible strain in the second group. This increases the number transcripts that could be
233 fine-mapped considerably, especially for large group sizes, see Figure 6A and Figure 6B. At the same
234 time, the distributions of number of fine-mapped variants are only marginally affected, see Figures 6E
235 and 6F. Nearly all high TV scores and/or high effect size and/or low *cis* eQTL p-value genes mentioned
236 by Mostafavi *et al.* can be fine-mapped (71 of 74), illustrating that MouseFM is particularly useful for
237 detecting variants and haplotypes that are compatible with binary, high effect phenotypes.

238 **Albinism**

239 Albinism is the absence of pigmentation resulting from a lack of melanin and is well-studied in mice (Beer-
240 mann *et al.*, 2004). It is a monogenic trait caused by a mutation in the *Tyr* gene (Beermann *et al.*, 2004),
241 which encodes for tyrosinase, an enzyme involved in melanin synthesis. The *Tyr* locus has been used
242 before for the validation of *in silico* fine-mapping approaches (Cervino *et al.*, 2007). According to
243 the Jackson Laboratory website (<https://www.jax.org>), 10 of the 37 inbred mouse strains are
244 albinos with a *Tyr^c* genotype (<http://www.informatics.jax.org/allele/MGI:1855976>),
245 see Figure 5A.

246 Our algorithm resulted in only one genetic locus, which includes the *Tyr* gene; only 245 SNPs have
247 different alleles between the albino and non-albino inbred mouse strains, all located from 7:83,244,464
248 to 7:95,801,713 (GRCm38). When removing SNPs except those of moderate or high impact, only one
249 variant remains. This variant rs31191169 at position 7:87,493,043, with reference allele C and with
250 alternative allele G in the albino strains is the previously described causal missense SNP in the *Tyr* gene,
251 which results in a cysteine to serine amino acid change at position 103 of the tyrosine protein.

252 **Interfrontal bone**

253 Further, we applied our algorithm to the phenotype of interfrontal bone formation, a complex skeletal
254 trait residing between the frontal bones in inbred mice (Figure 5B). In some inbred mouse strains, the
255 interfrontal bone is present or absent in all mice, whereas other strains are polymorphic for this phenotype
256 suggesting that phenotypic plasticity is involved. Phenotypic data related to interfrontal bone has recently
257 been generated by Zimmerman *et al.* (Zimmerman *et al.*, 2019) for 27 inbred mouse strains (Figure 5B).
258 They performed QTL mapping and identified four significant loci on chromosomes 4,7,11 and 14, the
259 same loci for interfrontal bone length and interfrontal bone width. For the genotyping, the authors use

260 the mapping and developmental analysis panel (MMDAP; Partners HealthCare Center for Personalized
261 Genetic Medicine, Cambridge, MA, United States), which contains 748 SNPs.

262 Of the available interfrontal bone data, we only used inbred strains for which all mice show the
263 same phenotype. This corresponds to four strains with interfrontal bone (C57BL/6J, C57L/J, CBA/J,
264 NZB/B1NJ) and five strains without interfrontal bone (C3H/HEJ, MOLF/EiJ, NZW/LacJ, WSB/EiJ,
265 SPRET/EiJ).

266 *In silico* fine-mapping resulted in 8,608 SNPs compatible with the observed interfrontal bone pheno-
267 type. Of these, 15 showed moderate or high impact on 12 candidate genes, see Table 1. None of the loci
268 identified by us overlaps with the markers of peak LOD score reported by Zimmerman *et al.*, but according
269 to visual inspection, two of their four QTL regions overlap with regions reported by MouseFM, one on
270 chromosome 7 and one on chromosome 11. MouseFM may thus have identified variants underlying
271 those two QTLs. The two other loci reported by Zimmerman *et al.* may have been missed by MouseFM,
272 because they are driven by strains not used here. Variant rs29393437 is located in the less well described
273 isoform ENSMUST00000131519.1 of *Stac2*, one of two isoforms of this gene. It is a missense variant,
274 changing arginine (R) to histidine (H) which is at low confidence predicted to be deleterious by SIFT.
275 *Stac2* has been shown to negatively regulate formation of osteoclasts, cells that dissect bone tissue (Jeong
276 *et al.*, 2018). *Phf21* is expressed during ossification of cranial bones in mouse early embryonic stages and
277 has been linked to craniofacial development (Kim *et al.*, 2012). Gene *Abcc6* is linked to abnormal snout
278 skin morphology in mouse and abnormality of the mouth, high palate in human according to MGI.

RSID	Position	Gene
rs32785405	1:36311963	<i>Arid5a</i>
rs27384937	2:92330761	<i>Phf21a</i>
rs32757904	7:45996764	<i>Abcc6</i>
rs32761224	7:46068710	<i>Nomo1</i>
rs32763636	7:46081416	<i>Nomo1</i>
rs13472312	7:46376829	<i>Myod1</i>
rs31674298	7:46443316	<i>Sergef</i>
rs31226051	7:49464827	<i>Nav2</i>
rs248206089	7:49547983	<i>Nav2</i>
rs45995457	9:86586988	<i>Me1</i>
rs29393437	11:98040971	<i>Stac2</i>
rs29414131	11:98042573	<i>Stac2</i>
rs251305478	11:98155926	<i>Med1</i>
rs27086373	11:98204403	<i>Cdk12</i>
rs27026064	11:98918145	<i>Cdc6</i>

Table 1. Moderate and high impact candidate variants and genes for interfrontal bone formation.

279 **Dystrophic cardiac calcification**

280 Physiological calcification takes place in bones, however pathologically calcification may affect the
281 cardiovascular system including vessels and the cardiac tissue. Dystrophic cardiac calcification (DCC) is
282 known as calcium phosphate deposits in necrotic myocardial tissue independently from plasma calcium
283 and phosphate imbalances. We previously reported the identification of four DCC loci *Dyscalc1*, *Dyscalc2*,
284 *Dyscalc3*, and *Dyscalc4* on chromosomes 7, 4, 12 and 14, respectively using QTL analysis and composite
285 interval mapping (Ivandic *et al.*, 1996, 2001). The *Dyscalc1* was confirmed as major genetic determinant
286 contributing significantly to DCC (Aherrahrou *et al.*, 2004). It spans a 15.2 Mb region on proximal
287 chromosome 7. Finally, chromosome 7 was further refined to a 80 kb region and *Abcc6* was identified
288 as causal gene (Meng *et al.*, 2007; Aherrahrou *et al.*, 2007). In this study we applied our algorithm to
289 previously reported data on 16 mouse inbred strains which were well-characterized for DCC (Aherrahrou
290 *et al.*, 2007). Eight inbred mouse strains were found to be susceptible to DCC (C3H/HeJ, NZW/LacJ,
291 129S1/SvImJ, C3H/HeH, DBA/1J, DBA/2J, BALB/cJ, NZB/B1NJ) and eight strains were resistant to
292 DCC (CBA/J, FVB/NJ, AKR/J, C57BL/10J, C57BL/6J, C57BL/6NJ, C57BR/cdJ, C57L/J). 2,003 SNPs
293 in 13 genetic loci were fine-mapped and found to match the observed DCC phenotype in the tested
294 16 DCC strains. Of these, 19 SNPs are moderate or high impact variants affecting protein amino acid

295 sequences of 13 genes localized in two chromosomal regions mainly on chromosome 7 (45.6-46.3 Mb)
 296 and 11 (102.4-102.6 Mb), see Table 2. The SNP rs32753988 is compatible with the observed phenotype
 297 manifestations and affects the previously identified causal gene *Abcc6*. This SNP has a SIFT score of 0.22,
 298 the lowest score after two SNPs in gene *Sec1* and one variant in gene *Mamstr*, although SIFT predicts all
 299 amino acid changes to be tolerated.

RSID	Position	Gene
rs46174746	7:45538428	<i>Plekha4</i>
rs49200743	7:45634990	<i>Rasip1</i>
rs32122777	7:45642384	<i>Mamstr</i>
rs215144870	7:45679109	<i>Sec1</i>
rs45768641	7:45679410	<i>Sec1</i>
rs51645617	7:45679423	<i>Sec1</i>
rs31997402	7:45725284	<i>Spaca4</i>
rs50753342	7:45794044	<i>Lmtk3</i>
rs50693551	7:45794821	<i>Lmtk3</i>
rs52312062	7:45798406	<i>Lmtk3</i>
rs49106901	7:45798469	<i>Emp3</i>
rs47934871	7:45918097	<i>Emp3</i>
rs32444059	7:45942897	<i>Ccdc114</i>
rs32753988	7:45998774	<i>Abcc6</i>
rs32778283	7:46219386	<i>Ush1c</i>
rs31889971	7:46288929	<i>Otog</i>
rs50613184	11:102456258	<i>Itga2b</i>
rs27040377	11:102457490	<i>Itga2b</i>
rs29383996	11:102605308	<i>Fzd2</i>

Table 2. Moderate and high impact candidate variants and genes for dystrophic cardiac calcification.

300 DISCUSSION

301 With MouseFM, we developed a novel tool for *in silico*-based genetic fine-mapping exploiting the
 302 extremely high homozygosity rate of inbred mouse strains for identifying new candidate SNPs and genes.
 303 Towards this, by including latest genotype data for 37 inbred mouse strains at a genome-wide scale derived
 304 from next generation sequencing, MouseFM uses the most detailed genetic resolution for this approach to
 305 date.

306 Using two large expression data sets, we apply MouseFM to more than 20,000 expression phenotypes
 307 of diverse distributions, using different minimum group sizes and also allowing up to one incompatible
 308 strain per group. This results in a comprehensive characterization of MouseFM fine-mapped candidate
 309 variants. For low group sizes, many phenotype compatible variants can be detected, but these likely
 310 include many more false-positives than larger group sizes. For larger group sizes, previously identified
 311 eQTLs of Mostafavi et al. (2014) are much more often successfully fine-mapped than expected by chance,
 312 which is in line with theoretical expectation that a given 10/10 group split is rather unlikely to be observed
 313 by chance and thus indicates a causal genetic effect. The high number of non-eQTL transcripts that
 314 could be fine-mapped also at large group sizes could have several sources. Firstly, we analyze only 20
 315 strains compared to 39 strains analyzed by Mostafavi et al. (2014), so likely not all of their eQTLs still
 316 apply to the smaller set of strains used here. Secondly, previously undetected eQTLs may occur in this
 317 smaller set, which could be tested in future work by repeating the Mostafavi *et al.* analysis for the exact
 318 same strains used by MouseFM. Lastly, these may indeed be chance findings unrelated to the expression
 319 phenotype, possibly confounded by strain kinship. Manual inspection would help to obtain a clearer
 320 picture on a case-by-case basis. Finally, the number of fine-mapped variants varies greatly, so in many
 321 cases, additional regulatory information will still be needed to refine the candidate variant list.

322 By re-analyzing previously published fine-mapping studies for albinism and dystrophic cardiac
 323 calcification, we could show that MouseFM is capable of re-identifying causal SNPs and genes. Re-
 324 analyzing a study on interfrontal bone formation (IF) resulted in MouseFM loci that did not overlap the

325 overall markers of peak LOD score reported in the original study, but according to visual inspection,
326 two of the corresponding QTLs. With gene *Stac2* we suggest a new candidate gene possibly affecting
327 interfrontal bone formation.

328 We selected cases studies particularly to validate that MouseFM can identify experimentally validated
329 variants and genes, such as the *Tyr* variant rs31191169 for albinism and the gene *Abcc6* for dystrophic
330 cardiac calcification. Variant rs31191169 is not a candidate variant and *Abcc6* not a candidate gene, both
331 are experimentally validated to be causally linked to the phenotype. Only for traits that are polygenic, e.g.
332 for DCC (but not for albinism), other candidates returned by MouseFM may be linked to the phenotype,
333 but they do not need to, they are only candidates to follow up on. A different type of case study relates to
334 phenotype interfrontal bone formation, for which causal variants and genes are not known. Still, several
335 candidate genes returned by MouseFM are plausible to affect the phenotype. In summary, additional DCC
336 candidate loci beyond *Abcc6* as well as identified interfrontal bone loci are valid candidate loci. Whether
337 they are in fact affecting the phenotypes needs to be assessed in subsequent QTL and experimental studies.

338 MouseFM performs most powerful and without limitations for Mendelian traits such as albinism.
339 Secondly, it is most useful as a second-line after QTL mapping. MouseFM is specifically designed to
340 accommodate this fine-mapping setting by allowing to provide start and end of a region to be analyzed.
341 Complex traits and phenotypes with several large effect loci are much more challenging. For these,
342 binarizing the phenotype and performing fine-mapping with MouseFM is not guaranteed to include all
343 causal variants and genes (unlike Mendelian traits). For this reason, we added the option to allow for
344 a user-selected number of outlier strains, which have a genotype discordant with the phenotype. The
345 rationale behind this is identification of genomic regions which are more similar in those strains showing
346 the phenotype compared to strains not showing the phenotype. Lastly, another informative MouseFM
347 setting is the comparison of one phenotype-outlier strain with all other strains, which identifies genetic
348 variants specific to this strain. In summary, MouseFM users need to consider that for polygenic and
349 complex traits, the quality of variant and gene candidates obtained by MouseFM depends on the number
350 and effect size and direction of loci, the genetic diversity of mouse strains and the variability of the
351 phenotype.

352 A current limitation of MouseFM is that it does only consider single nucleotide variants. Loci
353 containing other types of genetic variation such as insertions, deletions or other, structural variants
354 affecting a phenotype may thus be missed. QTL studies would be able to identify these loci. This could
355 thus be a reason for QTLs without MouseFM support, such as we observe in our case study on interfrontal
356 bone formation. However, this constitutes not a methodological limitation, and other variant types can be
357 added to MouseFM. To date though, genome-wide identification of structural variants is less accurate and
358 less standard compared to small variant identification and thus structural variants are typically not yet
359 systematically analyzed in genetic studies.

360 We observe that frequently genetic loci identified by MouseFM fine-mapping consist of few or often
361 only a single variant compatible with the phenotype. For example, five of 13 fine-mapped DCC loci
362 comprise a single phenotype-pattern compatible variant and 3 loci comprise less than 10 variants. This
363 contradicts the expectation that commonly used mice strains differ by chromosomal segments comprising
364 several or many consecutive variants. Commonly used inbred strains display mosaic genomes with
365 sequences from different subspecific origins (Wade et al., 2002) and thus one may expect genomic regions
366 with high SNP rate. Fine-mapped loci comprising more phenotype-compatible variants are thus likely
367 more informative for downstream experiments. When allowing no phenotype outlier strain (i.e. $\text{thr1}=0$ and
368 $\text{thr2}=0$), in the case of DCC we identify only six such genetic loci that lend themselves for further experi-
369 mental fine-mapping (chr7:45,327,763-46,308,368 (811 compatible SNVs); chr7:54,894,131-54,974,260
370 (32 compatible SNVs); chr9:106,456,180-106,576,076 (170 SNVs); chr11:24,453,006-24,568,761 (40
371 compatible SNVs); chr11:102,320,611-102,607,848 (46 compatible SNVs); chr16:65,577,755-66,821,071
372 (890 compatible SNVs)).

373 CONCLUSIONS

374 We show here that *in silico* fine-mapping can effectively identify genetic loci compatible with the observed
375 phenotypic differences and prioritize genetic variants and genes for further consideration. This allows for
376 subsequent more targeted approaches towards identification of causal variants and genes using literature,
377 data integration, and lab and animal experiments. MouseFM *in silico* fine-mapping provides phenotype-
378 compatible genotypic differences between representatives of many common laboratory mice strains. These

379 genetic differences can be used to select strains which are genetically diverse at an indicated genetic locus
 380 and which are thus providing additional information when performing phenotyping or breeding-based
 381 mouse experiments. Thus *in silico* fine-mapping is a first, very efficient step on the way of unraveling
 382 genotype-phenotype relationships.

383 During the implementation of MouseFM we have paid attention to a very easy handling. To perform a
 384 fine-mapping study, our tool only requires binary information (e.g. case versus control) for a phenotype of
 385 interest on at least two of the 37 available input strains. Further optional parameters can be set to reduce
 386 or expand the search space. MouseFM can also be performed on quantitative traits as we showed for
 387 expression data and in the interfrontal bone example.

388 The general approach underlying MouseFM is straightforward and it has been successfully applied
 389 before in a case-wise setting (Liao et al., 2004; Zheng et al., 2012; Hall and Lammert, 2017; Mulligan et al.,
 390 2019) and also recently in a high-throughput manner (Arslan et al., 2020). Nonetheless, genome-wide
 391 variant data of many inbred mouse strains is quite recently available, and this data is large and from
 392 raw VCF format difficult to assess systematically for any phenotype of interest. MouseFM is the first
 393 tool providing this functionality together with versatile query settings and subsequent variant and gene
 394 annotation and filtering options.

395 In conclusion, MouseFM implements a conceptually simple, but powerful approach for *in silico*
 396 fine-mapping including a very comprehensive SNV set of 37 inbred mouse strains. By re-analyzing
 397 three fine-mapping studies, we demonstrate that MouseFM is a very useful tool for studying genotype-
 398 phenotype relationships in mice. Further, by high-throughput analysis of all genes of two expression
 399 datasets, we illustrate that MouseFM is capable of analyzing molecular phenotypes in a versatile and
 400 high-throughput manner. This shows the potential of MouseFM to be used for large-scale analyses of
 401 diverse phenotypes in future work.

402 REFERENCES

- 403 Aherrahrou, Z., Axtner, S. B., Kaczmarek, P. M., Jurat, A., Korff, S., Doehring, L. C., Weichenhan, D.,
 404 Katus, H. A., and Ivandic, B. T. (2004). A locus on chromosome 7 determines dramatic up-regulation
 405 of osteopontin in dystrophic cardiac calcification in mice. *The American Journal of Pathology*,
 406 164(4):1379–1387.
- 407 Aherrahrou, Z., Doehring, L. C., Kaczmarek, P. M., Liptau, H., Ehlers, E.-M., Pomarino, A., Wrobel,
 408 S., Götz, A., Mayer, B., Erdmann, J., and Schunkert, H. (2007). Ultrafine mapping of *Dyscalc1* to
 409 an 80-kb chromosomal segment on chromosome 7 in mice susceptible for dystrophic calcification.
 410 *Physiological Genomics*, 28(2):203–212.
- 411 Arslan, A., Guan, Y., Chen, X., Donaldson, R., Zhu, W., Ford, M., Wu, M., Zheng,
 412 M., Dill, D. L., and Peltz, G. (2020). High Throughput Computational Mouse
 413 Genetic Analysis. *bioRxiv*. Publisher: Cold Spring Harbor Laboratory .eprint:
 414 <https://www.biorxiv.org/content/early/2020/09/01/2020.09.01.278465.full.pdf>.
- 415 Ashbrook, D. G., Arends, D., Prins, P., Mulligan, M. K., Roy, S., Williams, E. G., Lutz, C. M., Valenzuela,
 416 A., Bohl, C. J., Ingels, J. F., McCarty, M. S., Centeno, A. G., Hager, R., Auwerx, J., Lu, L., and
 417 Williams, R. W. (2021). A Platform for Experimental Precision Medicine: The Extended BXD Mouse
 418 Family. *Cell Systems*.
- 419 Beermann, F., Orlow, S. J., and Lamoreux, M. L. (2004). The Tyr (albino) locus of the laboratory
 420 mouse. *Mammalian Genome: Official Journal of the International Mammalian Genome Society*,
 421 15(10):749–758.
- 422 Bogue, M. A., Grubb, S. C., Walton, D. O., Philip, V. M., Kolishovski, G., Stearns, T., Dunn, M. H.,
 423 Skelly, D. A., Kadakkuzha, B., TeHennepe, G., Kunde-Ramamoorthy, G., and Chesler, E. J. (2018).
 424 Mouse Phenome Database: an integrative database and analysis suite for curated empirical phenotype
 425 data from laboratory mice. *Nucleic Acids Research*, 46(D1):D843–D850.
- 426 Cervino, A. C. L., Darvasi, A., Fallahi, M., Mader, C. C., and Tsinoremas, N. F. (2007). An integrated *in*
 427 *silico* gene mapping strategy in inbred mice. *Genetics*, 175(1):321–333.
- 428 Dickinson, M. E., Flenniken, A. M., Ji, X., Teboul, L., Wong, M. D., White, J. K., Meehan, T. F., Weninger,
 429 W. J., Westerberg, H., Adissu, H., Baker, C. N., Bower, L., Brown, J. M., Caddle, L. B., Chiani, F., Clary,
 430 D., Cleak, J., Daly, M. J., Denegre, J. M., Doe, B., Dolan, M. E., Edie, S. M., Fuchs, H., Gailus-Durner,
 431 V., Galli, A., Gambadoro, A., Gallegos, J., Guo, S., Horner, N. R., Hsu, C.-W., Johnson, S. J., Kalaga,
 432 S., Keith, L. C., Lanoue, L., Lawson, T. N., Lek, M., Mark, M., Marschall, S., Mason, J., McElwee,

- 433 M. L., Newbigging, S., Nutter, L. M. J., Peterson, K. A., Ramirez-Solis, R., Rowland, D. J., Ryder, E.,
434 Samocha, K. E., Seavitt, J. R., Selloum, M., Szoke-Kovacs, Z., Tamura, M., Trainor, A. G., Tudose,
435 I., Wakana, S., Warren, J., Wendling, O., West, D. B., Wong, L., Yoshiki, A., International Mouse
436 Phenotyping Consortium, Jackson Laboratory, Infrastructure Nationale PHENOMIN, Institut Clinique
437 de la Souris (ICS), Charles River Laboratories, MRC Harwell, Toronto Centre for Phenogenomics,
438 Wellcome Trust Sanger Institute, RIKEN BioResource Center, MacArthur, D. G., Tocchini-Valentini,
439 G. P., Gao, X., Flicek, P., Bradley, A., Skarnes, W. C., Justice, M. J., Parkinson, H. E., Moore, M.,
440 Wells, S., Braun, R. E., Svenson, K. L., de Angelis, M. H., Herculat, Y., Mohun, T., Mallon, A.-M.,
441 Henkelman, R. M., Brown, S. D. M., Adams, D. J., Lloyd, K. C. K., McKerlie, C., Beaudet, A. L.,
442 Bućan, M., and Murray, S. A. (2016). High-throughput discovery of novel developmental phenotypes.
443 *Nature*, 537(7621):508–514.
- 444 Doran, A. G., Wong, K., Flint, J., Adams, D. J., Hunter, K. W., and Keane, T. M. (2016). Deep genome
445 sequencing and variation analysis of 13 inbred mouse strains defines candidate phenotypic alleles,
446 private variation and homozygous truncating mutations. *Genome Biology*, 17(1):167.
- 447 Eilbeck, K., Lewis, S. E., Mungall, C. J., Yandell, M., Stein, L., Durbin, R., and Ashburner, M. (2005).
448 The Sequence Ontology: a tool for the unification of genome annotations. *Genome Biology*, 6(5):R44.
- 449 Grupe, A., Germer, S., Usuka, J., Aud, D., Belknap, J. K., Klein, R. F., Ahluwalia, M. K., Higuchi, R.,
450 and Peltz, G. (2001). In silico mapping of complex disease-related traits in mice. *Science (New York,
451 N.Y.)*, 292(5523):1915–1918.
- 452 Hall, R. A. and Lammert, F. (2017). Systems Genetics of Liver Fibrosis. *Methods in Molecular Biology*
453 (*Clifton, N.J.*), 1488:455–466.
- 454 Hunt, S. E., McLaren, W., Gil, L., Thormann, A., Schuilenburg, H., Sheppard, D., Parton, A., Armean,
455 I. M., Trevanion, S. J., Flicek, P., and Cunningham, F. (2018). Ensembl variation resources. *Database:
456 The Journal of Biological Databases and Curation*, 2018.
- 457 Ivandic, B. T., Qiao, J. H., Machleder, D., Liao, F., Drake, T. A., and Lusis, A. J. (1996). A locus on
458 chromosome 7 determines myocardial cell necrosis and calcification (dystrophic cardiac calcinosis) in
459 mice. *Proceedings of the National Academy of Sciences of the United States of America*, 93(11):5483–
460 5488.
- 461 Ivandic, B. T., Utz, H. F., Kaczmarek, P. M., Aherrahrou, Z., Axtner, S. B., Klepsch, C., Lusis, A. J.,
462 and Katus, H. A. (2001). New Dyscalc loci for myocardial cell necrosis and calcification (dystrophic
463 cardiac calcinosis) in mice. *Physiological Genomics*, 6(3):137–144.
- 464 Jeong, E., Choi, H. K., Park, J. H., and Lee, S. Y. (2018). STAC2 negatively regulates osteoclast formation
465 by targeting the RANK signaling complex. *Cell Death and Differentiation*, 25(8):1364–1374.
- 466 Keane, T. M., Goodstadt, L., Danecek, P., White, M. A., Wong, K., Yalcin, B., Heger, A., Agam, A.,
467 Slater, G., Goodson, M., Furlotte, N. A., Eskin, E., Nellåker, C., Whitley, H., Cleak, J., Janowitz, D.,
468 Hernandez-Pliego, P., Edwards, A., Belgard, T. G., Oliver, P. L., McIntyre, R. E., Bhomra, A., Nicod,
469 J., Gan, X., Yuan, W., van der Weyden, L., Steward, C. A., Bala, S., Stalker, J., Mott, R., Durbin, R.,
470 Jackson, I. J., Czechanski, A., Guerra-Assunção, J. A., Donahue, L. R., Reinholdt, L. G., Payseur,
471 B. A., Ponting, C. P., Birney, E., Flint, J., and Adams, D. J. (2011). Mouse genomic variation and its
472 effect on phenotypes and gene regulation. *Nature*, 477(7364):289–294.
- 473 Kim, H.-G., Kim, H.-T., Leach, N. T., Lan, F., Ullmann, R., Silahtaroglu, A., Kurth, I., Nowka, A.,
474 Seong, I. S., Shen, Y., Talkowski, M. E., Ruderfer, D., Lee, J.-H., Glotzbach, C., Ha, K., Kjaergaard, S.,
475 Levin, A. V., Romeike, B. F., Kleefstra, T., Bartsch, O., Elsea, S. H., Jabs, E. W., MacDonald, M. E.,
476 Harris, D. J., Quade, B. J., Ropers, H.-H., Shaffer, L. G., Kutsche, K., Layman, L. C., Tommerup,
477 N., Kalscheuer, V. M., Shi, Y., Morton, C. C., Kim, C.-H., and Gusella, J. F. (2012). Translocations
478 disrupting PHF21A in the Potocki-Shaffer-syndrome region are associated with intellectual disability
479 and craniofacial anomalies. *American Journal of Human Genetics*, 91(1):56–72.
- 480 Liao, G., Wang, J., Guo, J., Allard, J., Cheng, J., Ng, A., Shafer, S., Puech, A., McPherson, J. D., Foernzler,
481 D., Peltz, G., and Usuka, J. (2004). In silico genetics: identification of a functional element regulating
482 H2-Ealpha gene expression. *Science (New York, N.Y.)*, 306(5696):690–695.
- 483 McLaren, W., Gil, L., Hunt, S. E., Riat, H. S., Ritchie, G. R. S., Thormann, A., Flicek, P., and Cunningham,
484 F. (2016). The Ensembl Variant Effect Predictor. *Genome Biology*, 17(1):122.
- 485 Meehan, T. F., Conte, N., West, D. B., Jacobsen, J. O., Mason, J., Warren, J., Chen, C.-K., Tudose,
486 I., Relac, M., Matthews, P., Karp, N., Santos, L., Fiegel, T., Ring, N., Westerberg, H., Greenaway,
487 S., Sneddon, D., Morgan, H., Codner, G. F., Stewart, M. E., Brown, J., Horner, N., International

- 488 Mouse Phenotyping Consortium, Haendel, M., Washington, N., Mungall, C. J., Reynolds, C. L.,
489 Gallegos, J., Gailus-Durner, V., Sorg, T., Pavlovic, G., Bower, L. R., Moore, M., Morse, I., Gao, X.,
490 Tocchini-Valentini, G. P., Obata, Y., Cho, S. Y., Seong, J. K., Seavitt, J., Beaudet, A. L., Dickinson,
491 M. E., Herault, Y., Wurst, W., de Angelis, M. H., Lloyd, K. C. K., Flenniken, A. M., Nutter, L. M. J.,
492 Newbigging, S., McKerlie, C., Justice, M. J., Murray, S. A., Svenson, K. L., Braun, R. E., White,
493 J. K., Bradley, A., Flicek, P., Wells, S., Skarnes, W. C., Adams, D. J., Parkinson, H., Mallon, A.-M.,
494 Brown, S. D. M., and Smedley, D. (2017). Disease model discovery from 3,328 gene knockouts by
495 The International Mouse Phenotyping Consortium. *Nature Genetics*, 49(8):1231–1238.
- 496 Meng, H., Vera, I., Che, N., Wang, X., Wang, S. S., Ingram-Drake, L., Schadt, E. E., Drake, T. A., and
497 Lusic, A. J. (2007). Identification of *Abcc6* as the major causal gene for dystrophic cardiac calcification
498 in mice through integrative genomics. *Proceedings of the National Academy of Sciences of the United*
499 *States of America*, 104(11):4530–4535.
- 500 Mostafavi, S., Ortiz-Lopez, A., Bogue, M. A., Hattori, K., Pop, C., Koller, D., Mathis, D., Benoist, C.,
501 and Immunological Genome Consortium (2014). Variation and genetic control of gene expression in
502 primary immunocytes across inbred mouse strains. *Journal of Immunology (Baltimore, Md.: 1950)*,
503 193(9):4485–4496.
- 504 Mulligan, M. K., Abreo, T., Neuner, S. M., Parks, C., Watkins, C. E., Houseal, M. T., Shapaker, T. M.,
505 Hook, M., Tan, H., Wang, X., Ingels, J., Peng, J., Lu, L., Kaczorowski, C. C., Bryant, C. D., Homanics,
506 G. E., and Williams, R. W. (2019). Identification of a Functional Non-coding Variant in the GABA A
507 Receptor $\alpha 2$ Subunit of the C57BL/6J Mouse Reference Genome: Major Implications for Neuroscience
508 Research. *Frontiers in Genetics*, 10:188.
- 509 Mulligan, M. K., Mozhui, K., Prins, P., and Williams, R. W. (2017). GeneNetwork: A Toolbox for
510 Systems Genetics. *Methods in Molecular Biology (Clifton, N.J.)*, 1488:75–120.
- 511 Uhl, E. W. and Warner, N. J. (2015). Mouse Models as Predictors of Human Responses: Evolutionary
512 Medicine. *Current Pathobiology Reports*, 3(3):219–223.
- 513 Wade, C. M., Kulbokas, E. J., Kirby, A. W., Zody, M. C., Mullikin, J. C., Lander, E. S., Lindblad-Toh, K.,
514 and Daly, M. J. (2002). The mosaic structure of variation in the laboratory mouse genome. *Nature*,
515 420(6915):574–578.
- 516 Yates, A., Beal, K., Keenan, S., McLaren, W., Pignatelli, M., Ritchie, G. R. S., Ruffier, M., Taylor,
517 K., Vullo, A., and Flicek, P. (2015). The Ensembl REST API: Ensembl Data for Any Language.
518 *Bioinformatics (Oxford, England)*, 31(1):143–145.
- 519 Zheng, M., Dill, D., and Peltz, G. (2012). A better prognosis for genetic association studies in mice.
520 *Trends in genetics: TIG*, 28(2):62–69.
- 521 Zimmerman, H., Yin, Z., Zou, F., and Everett, E. T. (2019). Interfrontal Bone Among Inbred Strains of
522 Mice and QTL Mapping. *Frontiers in Genetics*, 10:291.